

See discussions, stats, and author profiles for this publication at: <https://www.researchgate.net/publication/259314085>

Efficient Exciton Concentrators Built from Colloidal Core/Crown CdSe/CdS Semiconductor Nanoplatelets

ARTICLE in NANO LETTERS · DECEMBER 2013

Impact Factor: 13.59 · DOI: 10.1021/nl403746p · Source: PubMed

CITATIONS

20

READS

168

6 AUTHORS, INCLUDING:



Mickael D Tessier

Ghent University

14 PUBLICATIONS 343 CITATIONS

SEE PROFILE



Piernicola Spinicelli

Institut Pasteur

41 PUBLICATIONS 1,007 CITATIONS

SEE PROFILE



Gilles Patriarche

French National Centre for Scientific Research

545 PUBLICATIONS 6,355 CITATIONS

SEE PROFILE



Sandrine Ithurria

École Supérieure de Physique et de Chimie In...

34 PUBLICATIONS 744 CITATIONS

SEE PROFILE

Efficient Exciton Concentrators Built from Colloidal Core/Crown CdSe/CdS Semiconductor Nanoplatelets

Mickaël D. Tessier,[†] Piernicola Spinicelli,[†] Dorian Dupont,[†] Gilles Patriarche,[‡] Sandrine Ithurria,[†] and Benoit Dubertret^{*,†}

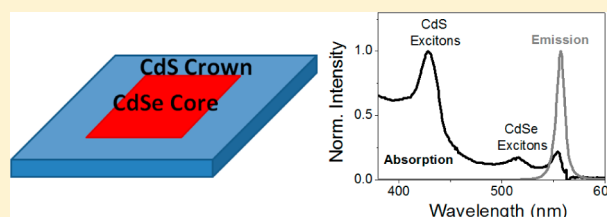
[†]Laboratoire de Physique et d'Etude des Matériaux, CNRS, Université Pierre et Marie Curie, ESPCI, 10 rue Vauquelin, 75005, Paris, France

[‡]Laboratoire Photonique et Nanostructures, CNRS, 91460, Marcoussis, France

S Supporting Information

ABSTRACT: We present the synthesis and the optical properties of a new type of two-dimensional heterostructure: core/crown CdSe/CdS nanoplatelets. They consist of CdSe nanoplatelets that are extended laterally with CdS. Both the CdSe core and the CdS crown dimensions can be controlled. Their thickness is controlled at the monolayer level. These novel nanoplatelet-based heterostructures have spectroscopic properties that can be similar to nanoplatelets or closer to quantum dots, depending on the CdSe core lateral size.

KEYWORDS: Nanoplatelets, heterostructure, nanosheets, quantum wells, 2D geometry, fluorescence



Significant advances have been made in the synthesis of colloidal semiconductor nanoparticles since the production of spherical nanocrystals, referred to as colloidal quantum dots (QDs), at the beginning of the 1990s.¹ For example, the shape of the nanoparticles can be finely controlled, and nanoparticles with various shapes such as tetrapods,² rods,³ or nanoplatelets (NPLs)^{4,5} have been synthesized. Shape control provides the opportunity to considerably change the electronic structure of nanoparticles of a given material. For instance, the charge carriers are confined in three dimensions (3D) in spheres, in two dimensions in nanorods, and in one dimension in NPLs. The composition of the nanoparticles can also be finely tuned, and various heterostructures have been synthesized. Such heterostructures are interesting because they provide a unique method to tune the charge carrier position using band edge engineering.⁶ They can also greatly enhance the fluorescence quantum yield and the photostability of core-only particles.⁷ It also leads to QDs that do not blink.^{8–10} Heterostructures have mainly been developed for spherical-, rod-, or tetrapod-shaped structures.^{11–15} For nanoplatelets, the first core/shell structures have only been introduced recently.^{16,17}

Here, we present the synthesis and optical properties of a new type of colloidal heterostructures: core/crown nanoplatelets (core/crown NPLs). They are anisotropic atomically flat colloidal heterostructures with a CdSe NPLs core surrounded in the lateral dimensions only by a CdS crown. Their two-dimensional structure is similar to colloidal NPLs: a thickness of a few nanometers and lateral dimensions that can achieve hundreds of nanometers. A core/crown NPL is then equivalent to a CdSe NPL included in a CdS NPL. The CdSe core NPLs and the CdS crown have the same exact number of atomic layers. We demonstrate that the core and the crown

dimensions can be controlled with precision. Depending on the CdSe core lateral dimensions, the core/crown NPLs with small core size can have spectral properties such as photon antibunching and dark state emission at low temperature similar to small CdSe/ZnS spherical QDs. On the opposite, when the CdSe core lateral dimensions are larger, the core/crown NPLs have spectroscopic behavior similar to CdSe NPLs: fast radiative lifetimes and absence of photon antibunching.

Core/crown NPLs are synthesized by a two-step method. The first step consists of a standard synthesis of a solution of a four monolayer (4 ML) thick CdSe NPLs.⁴ The absorption spectrum of these NPLs is presented in Figure 1a. The first two absorption maxima are the heavy-hole electron and the light-hole electron transitions. These NPLs have an emission spectrum with a maximum at 513 nm and a narrow line width, close to 8 nm, due to the pure 1D confinement. These CdSe NPLs are precipitated, washed, and used as seeds to be extended laterally in CdSe/CdS core/crown NPLs by continuous injection of cadmium and sulfur precursors. The sulfur precursor is made from elemental sulfur dissolved in octadecene, and the cadmium precursor is a mixture of cadmium acetate and oleic acid (cf. Materials and Methods). As for the lateral extension of CdSe NPLs,¹⁸ the presence of an acetate salt is necessary to obtain an extension with CdS. The core/crown CdSe/CdS NPLs have an emission spectra with the same maximum than the CdSe core-only NPLs. In contrast,

Received: October 8, 2013

Revised: December 3, 2013

Published: December 11, 2013

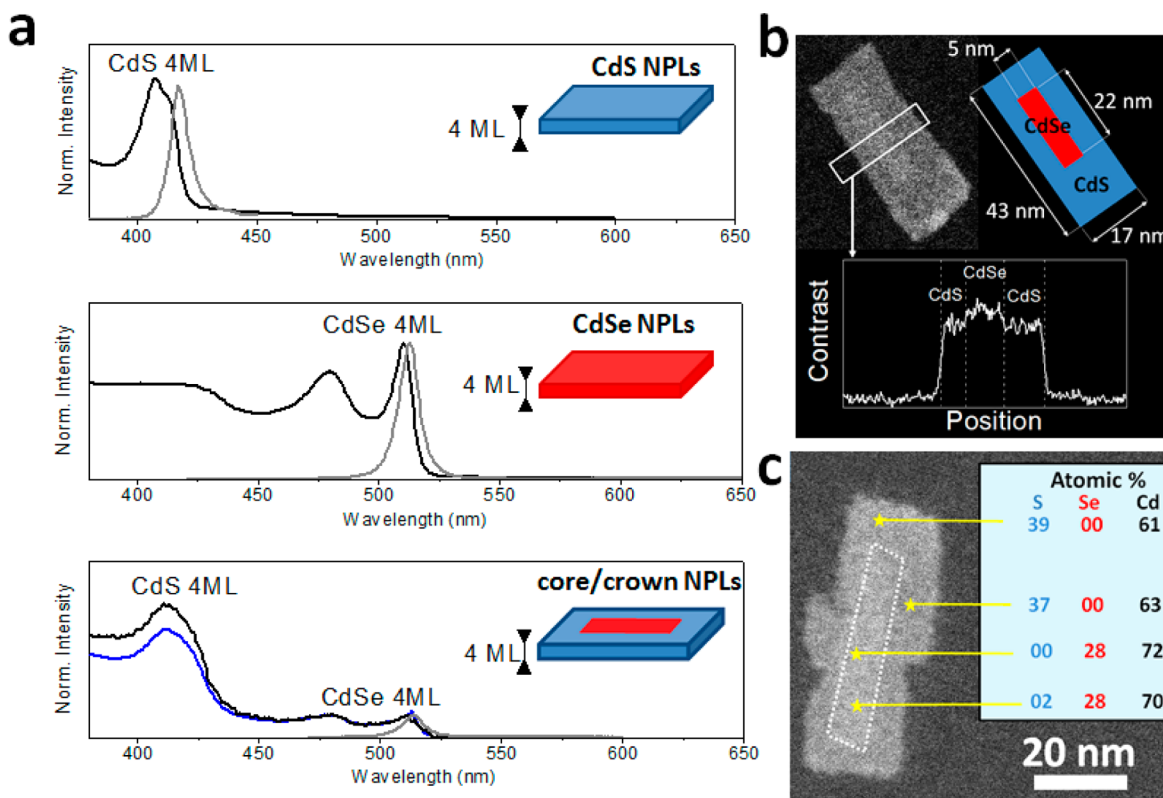


Figure 1. (a) Absorption (black) and emission (gray) spectra of CdS NPLs (top), CdSe NPLs (medium), and CdSe/CdS core/crown NPLs (bottom). Excitation spectrum (blue) at 514 nm of core/crown NPLs (bottom). Photoluminescence excitation and absorption spectra of core/crown NPLs are normalized at the CdSe light/hole transition (479 nm). All of these NPLs are 4 ML thick. (b) TEM image and contrast profile of a CdSe/CdS core/crown NPL. (c) Elemental analysis by EDX. Atomic percentages of Cd, S, and Se at different points of a CdSe/CdS core/crown NPL.

their photoluminescence excitation (PLE) spectrum differs from that of CdSe NPLs. While it contains the two excitons characteristic of the CdSe NPLs, it also contains two additional peaks, close to each other with maxima around 410 nm. These peaks, located at the same position than the light-hole electron and heavy-hole electron transition of 4 ML CdS NPLs (Figure 1a, top), are the spectroscopic signature of the 4 ML CdS crown around the CdSe core. The comparison between the absorption and the excitation spectra reveals that the solution is mostly composed of core/crown NPLs. However, this synthesis may generate a secondary nucleation of CdS NPLs, but with an optimization of the synthesis parameters (temperature, precursor's injection rate, concentration, and core size) it can be avoided (cf. Figure S1 in the Supporting Information). The structure of core/crown NPL is confirmed by transmission electron microscope (TEM) analysis. In high-angle annular dark-field (HAADF), core/crown NPLs appear as NPLs with a contrast difference between the core and the crown (Figure 1b). This contrast difference is consistent with the density difference between the sulfur and the selenium expected in adjacent 4 ML CdSe and CdS NPLs. The CdSe core appears in the center of a continuous CdS crown. Elementary analysis with energy-dispersive X-ray spectroscopy (EDX) in different points of a core/crown NPL confirms that the core is composed only of cadmium and selenium, whereas the crown is composed only of cadmium and sulfur (Figure 1c). This demonstrates that the CdS growth occurs only on the lateral edges of the CdSe NPLs, and not in the thickness. Both for the core and the crown, the elementary analysis reveals that the cadmium is in excess, as

expected since the large facets of the NPLs are cadmium planes passivated with carboxylate ligands. As a consequence, four monolayer thick core/crown NPLs have five cadmium crystal planes and four selenium (or sulfur) crystal planes in the thickness direction. During the writing of the manuscript, we became aware of a related work reporting the realization of heteronanoplatelets similar to the 4 ML (large)core/crown nanoplatelets and obtained through a different synthesis.¹⁹ However, both protocols use a high concentration of the acetate species to allow the anisotropic growth of CdS.

As we have the confirmation of the core/crown CdSe/CdS structure, some additional comments can be done on the spectroscopic data of Figure 1a. The absence of energy shift for both the heavy-hole electron and the light-hole electron transitions when comparing 4 ML thick core-only CdSe, core-only CdS, and CdSe/CdS core/crown NPLs confirms that the CdS growth occurs only in the lateral direction. Indeed, even a one-atom-thick change in the NPLs thickness produces very pronounced redshift of the exciton energy, as it was observed in core/shell NPLs.^{16,17,20} In core/crown NPLs, photons with energies higher than the CdS band gap are absorbed both by CdSe and CdS, but photoluminescence emission is only observed in the CdSe. This can be explained because of the valence band alignment between CdSe and CdS. CdSe/CdS is generally seen as a quasi-type II structure. The conduction band offset is not perfectly known and depends on the temperature,²¹ but the valence band offset is in general at least 400 meV.^{22–24} This leads to a rapid localization of the hole in the CdSe part of the heterostructure. Since the exciton

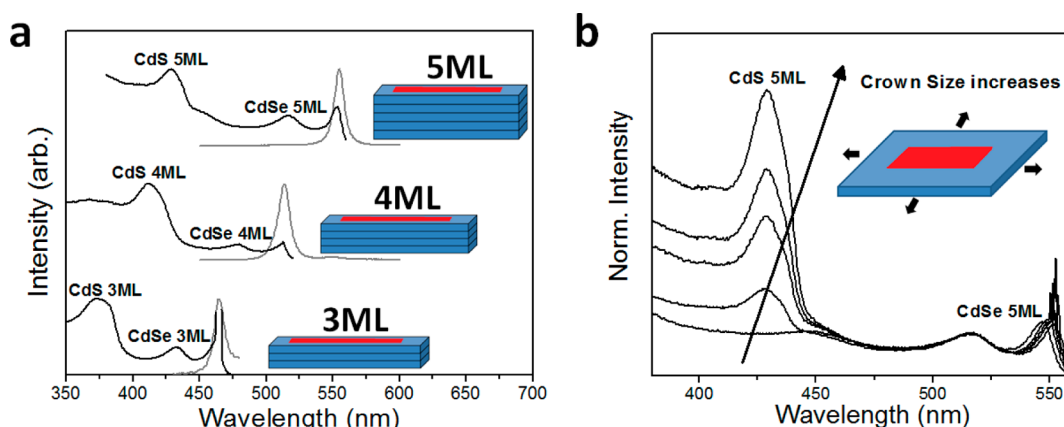


Figure 2. (a) Emission (gray) and excitation at the maximum of emission (black) spectra of CdSe/CdS core/crown NPLs with different thicknesses. (b) Excitation spectra at 552 nm of 5 ML thick CdSe/CdS core/crown NPLs with different crown sizes (31 nm \times 7 nm CdSe core-only, 35 nm \times 8 nm, 50 nm \times 9 nm, 70 nm \times 15 nm, 110 nm \times 20 nm).

binding energy in these ultrathin NPLs is very large, of the order of few hundreds of meV,²⁵ the electron is dragged with the hole in the CdSe core where the exciton can recombine. Consequently, because of this strong exciton binding energy, core/crown NPLs can be seen as a type-I structure. Then the electron–hole recombination occurs in the core in core/crown NPLs. In CdSe/CdS spherical QDs, the CdS shell growth induces a rapid redshift of the emission maximum because of the delocalization of the electron in the CdS shell. This delocalization results from the proximity of the CdSe and the CdS conduction bands. Even larger redshifts are observed when CdSe/CdS core/shell structures are made with a CdS growth in the NPL thickness direction. In the CdSe/CdS core/crown structures, the crown growth induces only a slight redshift of the emission, even for the extended CdS crown. This important difference most probably results from the exciton binding energy that exists in the core/crown 2D structures. Because the CdS crown is grown only laterally, the large binding energy that was computed in the case of core-only NPLs, and that results from the smaller dielectric constant of the media outside of the NPL, remains unaffected upon the CdS growth. In regular core/shell structures on the opposite, since the CdS grows in all directions, the exciton dielectric environment of the exciton changes upon CdS deposition. This results in a decrease of the exciton binding energy. These observations confirm the prediction in the seminal paper from Keldysh.²⁶

Core/crown CdSe/CdS NPLs can be synthesized in pure population with different thicknesses. As for the core-only NPLs, these thicknesses are controlled with atomic precision. In Figure 2a, emission and excitation spectra of three populations of nanoplatelets with different thickness are represented. These populations have both CdSe and CdS excitons for which the energy positions are close to the core-only values (cf. Table 1). This demonstrates that the core and the crown have exactly the same thickness that can be tuned at the monolayer level. The crown lateral extension can be tuned during the second step of the core/crown synthesis, during the continuous injection of CdS precursors. Typically, the size of the crown is controlled by the quantity of precursors injected in the solution. In Figure 2b, emission and excitation spectra of solutions of core/crown NPLs with five monolayer thickness and different crown sizes are represented. In this figure, the core/crown NPLs lateral dimensions range from 7 nm \times 31 nm (core-only NPLs) to 20 nm \times 110 nm (core/crown NPLs). As

Table 1. Absorption Maxima of Excitonic Transitions (nm) of CdS, CdSe and Core/Crown NPLs with Different Thicknesses

thickness	transition	core/crown NPLs			
		CdS NPLs	CdS excitons	CdSe excitons	CdSe NPLs
3 ML	light hole–electron	373	372	432	434
	heavy hole–electron	382	382	463	462
4 ML	light hole–electron	408	410	479	478
	heavy hole–electron	415	418	511	510
5 ML	light hole–electron	430	429	516	518
	heavy hole–electron	437	436	553	550

the crown size increases, the CdS excitons become more and more dominant. When the crown size becomes too large, some cracks appear on core/crown NPLs (cf. Figure S2 in Supporting Information). The cracks' appearance is correlated with the presence of CdS NPLs in the mixture. As this secondary population has the same thickness than the synthesized core/crown NPLs, we suggest that they may be chunks of crown which break off.

We now turn to the synthesis of core/crown NPLs with different core lateral sizes. The core lateral extension can be adjusted using two different techniques. During the CdSe nanoplatelets synthesis, the reaction conditions can be tuned so that NPLs with small lateral dimensions are obtained. With this technique, we could obtain CdSe NPLs with lateral dimensions as small as 4 nm \times 20 nm. To obtain CdSe NPLs with smaller lateral sizes, we injected the cadmium and the sulfur precursors as soon as the CdSe NPLs seeds have formed. Although this procedure does not rule out the formation of a composition gradient between the core and the shell, it yields to CdSe NPLs with lateral dimensions of just few nanometers. In addition, secondary population of CdS NPLs is avoided with this protocol (cf. Figure S3 in the Supporting Information). In Figure 3, we present TEM and spectroscopic characterization of these CdSe/CdS core/crown NPLs with cores of very small lateral dimensions. In HAADF, the CdSe cores are not visible, most probably because their lateral dimensions are too small.

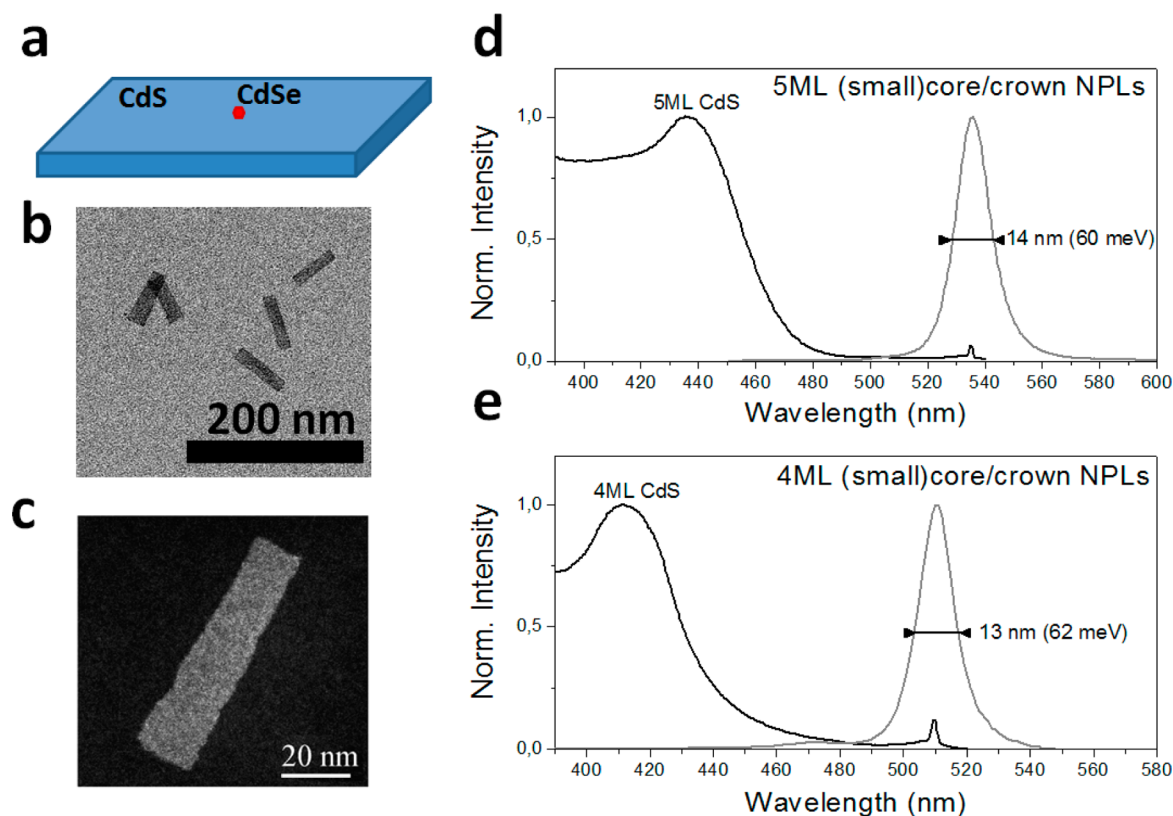


Figure 3. (a) Representative scheme of CdSe/CdS (small)core/crown NPLs. (b) TEM image of 5 ML thick (small)core/crown NPLs. (c) HAADF TEM image of a 5 ML thick (small)core/crown NPL (d and e) Emission (gray) and excitation at the maximum of emission (black) spectra of two populations of (small)core/crown NPLs with different thickness.

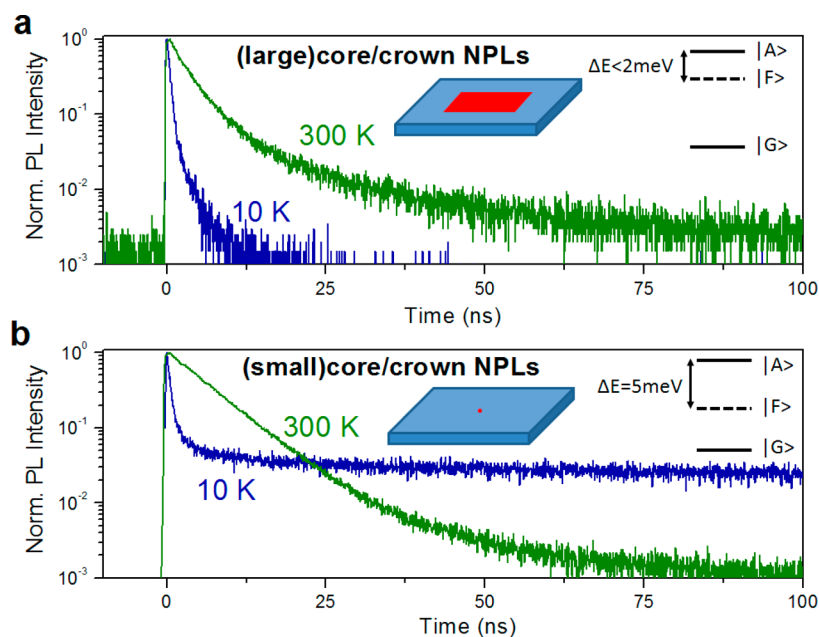


Figure 4. Time-resolved fluorescence spectroscopy at room and cryogenic temperature on core/crown nanoparticles with cores of different lateral sizes and schematic energy level position of authorized $|A\rangle$, forbidden $|F\rangle$, and ground $|G\rangle$ states. (a) (Large)core/crown NPLs and (b) (small)core/crown QDs.

The PLE spectra of these (small)core/crown NPLs is similar to the ones of (large)core/crown NPLs but with two notable differences. The first one is that the absorbance ratio between the CdS and the CdSe excitons is very large, much larger than in the case of (large)core/crown NPLs. This confirms that the

CdSe lateral dimensions are indeed very small compared to the ones of CdS. The second difference is that the emission line width of the (small)core/crown is larger than that of (large)core/crown NPLs. The quantum yield of (small)core/crown NPLs can be achieved 60%. Interestingly, while CdS

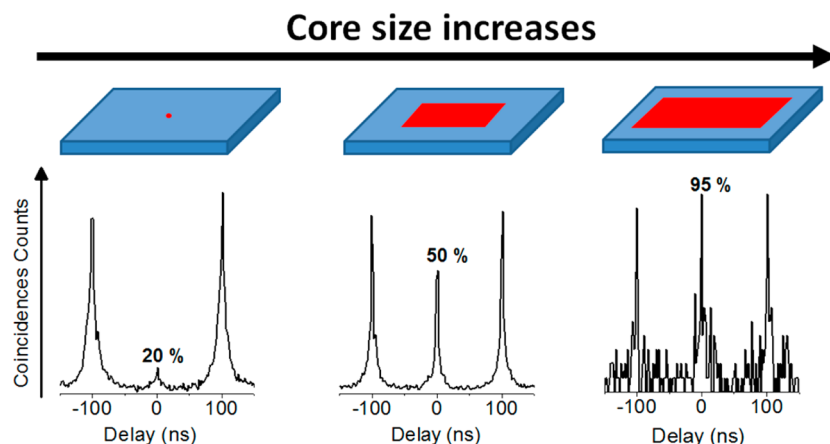


Figure 5. Photon coincidences diagram for (small)core/crown NPLs, (medium)core/crown NPLs, and (large)core/crown NPLs.

nanoplatelets are generally blended and aggregated,⁴ the core/crown QDs are typically deposited lay flat on the TEM grid and can be easily observed individually. We synthesized two pure populations of (small)core/crown NPLs with different thicknesses: 4 ML (Figure 3e) and 5 ML (Figure 3d). The spectral lines of these two populations are much narrower compared to the lines of CdSe spherical nanocrystals but are larger than the lines of CdSe nanoplatelets. A typical solution of CdSe nanocrystals emitting around these wavelengths has a line width of 100 meV (25 nm). The line width of a nanoplatelet solution is typically around 35 meV (8 nm).⁴ For core/crown QDs, the line width is around ~60 meV (13–14 nm). We performed single (small)core/crown NPLs emission spectra to check if their larger line width compare to NPLs is due to inhomogeneous broadening because of dispersion between each particles or if it is an intrinsic phenomenon (cf. Figure S4 in the Supporting Information). The line width of a single (small)core/crown NPLs is 50 meV (11.5 nm). This value is slightly smaller to the line width of the solution of (small)core/crown NPLs (60 meV, 13–14 nm), but it is larger to the line width of core-only or (large)core/crown nanoplatelets (37 meV, 8 nm). Interestingly the line width is the same as the one measured for single CdSe QDs.²⁷ These results suggest that some dispersity between (small)core/crown NPLs tend to enlarge slightly the line width of the fluorescence spectrum of the solution but they also have an intrinsic larger line width compared to (large)core/crown NPLs.

We now present time-resolved spectroscopy of core/crown NPLs for different CdSe lateral sizes. We observe strong differences in fluorescence lifetime evolution with temperature between different core sizes (cf. Figure 4). For (large)core/crown NPLs, the fluorescence lifetime is shortening as the temperature is decreases. At 10 K, an average fluorescence lifetime of 200–300 ps is measured. The lifetime shortening is concomitant with an increase of the fluorescence intensity (see Figure S5 in the Supporting Information). This fluorescence behavior is similar to the one observed for CdSe NPLs.^{4,28} We observe a completely different evolution for (small)core/crown NPLs. When the temperature decreases, the fluorescence lifetime becomes longer, and the intensity decreases slightly (Figure S5 in Supporting Information). At 10 K, the intensity decay can be fitted by a biexponential curve with a short component of 1.4 ns (10% of the emitted photons) and a very long lifetime of 380 ns (90% of the emitted photons). This behavior is similar to that observed for colloidal quantum

dots.^{29–31} The biexponential lifetime is attributed to the presence of two emissive states in the exciton fine structure: an authorized state $|A\rangle$ with a large oscillator strength, and short lifetime, and a forbidden state $|F\rangle$ with a small oscillator strength and long lifetime. When the temperature decreases, the exciton is trapped in the forbidden state $|F\rangle$ which leads to the appearance of a long fluorescence lifetime. We estimated the energy gap between $|F\rangle$ and $|A\rangle$ state²⁹ with a fit of the intensity decay at different temperatures (see Figure S6 in Supporting Information), and we found 5 meV, a value close to the one found for CdSe/ZnS core/shell QDs with a radius of 1.5 nm.²⁹ This spectroscopic analysis confirms that the CdSe core in the (small)core/crown NPLs has indeed small lateral dimensions (a few nanometers). In the same way, we estimate that for (large)core/crown NPLs the energy gap is inferior to 2 meV. This explains why we do not observe the $|F\rangle$ states, since at 10 K there is still thermal equilibrium between the $|A\rangle$ and the $|F\rangle$ state.

Finally, a Hanbury Brown and Twist setup based on two photoavalanche photodiodes has been used to obtain coincidence diagram of the photon arrival time between the two detectors. This kind of setup can be used to check if single nanoparticles are single photon emitters.^{32,33} An interesting evolution of the coincidence diagram occurs with the change of the core size (Figure 5). For (small)core/crown NPLs, antibunched light with only 20% of photons arriving on both detectors for the same excitation pulse is measured. This quantity increases as the core size increases. For core/crown NPLs with a core of about 7 nm \times 31 nm, the portion of bunched photons is around 50%, and for a large core size of about 12 nm \times 45 nm the emitted light is classic (>90%), as expected in quantum well systems. This study brings yet another confirmation that in (small)core/crown NPLs the CdSe NPLs lateral dimensions are similar to those of CdSe quantum dots with 3D confinement.

In summary, we have demonstrated the synthesis of a novel type of CdSe/CdS heterostructures obtained from the lateral extension of CdSe NPLs with a CdS crown. We have shown that these 2D objects are atomically flat with CdS and CdSe parts that have exactly the same number of monolayers. We could synthesize three pure populations of these heterostructures with different thickness expressed in terms of monolayers. We have gathered spectroscopic data for these core/crown structures for different thickness and different core and crown size. When the CdSe core of these NPLs has lateral

dimensions similar to those already reported for CdSe NPLs core-only, the behavior is very similarly to the one of core-only NPLs. As the CdSe core lateral dimension gets smaller, some characteristics of 3D confined objects appear such as photon antibunching and dark state emission with a long lifetime of hundred of ns at cryogenic temperature.

In these core/crown structures, excitons collected by the CdS crown are transferred rapidly to the CdSe core thanks to the combined effect of the band alignment between the core and the shell and the large binding energy of the exciton. As a consequence, the CdS acts as an exciton funnel that collects the excitons and transfers them to the CdSe core. In contrast to CdSe/CdS core/shell structures, in these flat highly anisotropic CdSe/CdS core/crown heterostructures the emission does not redshift as the CdS crown grows. This observation is interpreted within the context of the increased binding energy in 2D structures due to the lower dielectric constant of the outer media, as first proposed by Keldysh in 1979.

Materials and Methods. *Chemicals.* Cadmium acetate dihydrate $\text{Cd}(\text{OAc})_2 \cdot 2\text{H}_2\text{O}$, technical grade 1-octadecene, oleic acid, myristic acid sodium salt, cadmium nitrate, and selenium in powder were purchased from Sigma Aldrich. Methanol, ethanol, toluene, and *n*-hexane were purchased from VWR.

Synthesis of Cadmium(myristate)₂. Cadmium nitrate (1.23 g) was dissolved in 40 mL of methanol. Then, 3.13 g of sodium myristate was dissolved in 250 mL of methanol (1 h with strong stirring). After complete dissolution, the two solutions were mixed, giving a white precipitate. This precipitate was filtered and washed on a Buchner vacuum flask and dried under vacuum for about 12 h.

Nanoplatelet Synthesis. Thicknesses were deduced from TEM measurements by Mahler et al.¹⁶

3 ML Thick NPLs (Emission at 463 nm). In a three-neck flask, 240 mg of $\text{Cd}(\text{Ac})_2$ (0.9 mmol), 150 μL of oleic acid (0.45 mmol), and 15 mL of octadecene were degassed under vacuum flow for 1 h at 80 °C. The mixture was then heated at 170 °C under argon flow, and a syringe of 150 μL of TOPSe at 1 M (0.15 mmol) was injected. The reaction is stopped after 10 min. NPLs are precipitated with ethanol and resuspended in hexane.

4 ML Thick NPLs (Emission at 512 nm). $\text{Cd}(\text{myr})_2$ (170 mg, 0.3 mmol), 12 mg (0.15 mmol) of Se, and 15 mL of ODE were introduced in a three-neck flask and were degassed under vacuum. The mixture was heated up to 240 °C under argon flow. At 195 °C, 80 mg of $\text{Cd}(\text{Ac})_2$ (0.30 mmol) were introduced. The mixture was heated for 10 min at 240 °C. At the end of the synthesis 0.5 mL of oleic acid was added to the solution. This synthesis produced 5 ML thick NPLs and also some spherical nanocrystals. The NPLs were separated from the nanocrystals using selective precipitation (hexane–ethanol 3:1). The NPLs were then dispersed in hexane.

5 ML Thick NPLs (Emission at 552 nm). $\text{Cd}(\text{myr})_2$ (170 mg, 0.3 mmol) and 14 mL of ODE were introduced in a three-neck flask and were degassed under vacuum. The mixture was heated under argon flow at 250 °C. A solution of 12 mg (0.15 mmol) of Se dispersed in 1 mL of ODE, prepared as described by Flamee et al.,³⁴ was quickly injected. One minute later, 120 mg of $\text{Cd}(\text{Ac})_2$ (0.45 mmol) was introduced. The mixture was heated for 10 min. At the end of the synthesis 0.5 mL of oleic acid was added to the solution. This synthesis produced 4 ML thick NPLs and also some spherical nanocrystals. The NPLs were separated from the nanocrystals using selective precip-

itation (hexane–ethanol 3:1). The NPLs were then dispersed in hexane.

Anisotropic Growth Mixture. A total of 480 mg of $\text{Cd}(\text{OAc})_2 \cdot 2\text{H}_2\text{O}$ (1.8 mmol) and 340 μL of oleic acid (1 mmol) was dissolved into 2 mL of ODE and heated up at 150 °C under air during 15 min under sustained stirring. The solution is regularly sonicated. Heating was stopped when the mixture was a gray and homogeneous gel. A portion of 3 mL of S dissolved in ODE at 0.1 M was added into the solution and kept stirred until injection.

Synthesis of (Large)Core/Crown NPLs. The entire product of a CdSe NPLs synthesis was put with 5 mL of ODE in a three-neck flask. The anisotropic growth mixture was injected continuously in the NPLs solution at 8 mL/h at 240 °C under argon flow. The secondary nucleation of CdS NPLs was favored by CdSe NPLs with large lateral sizes, a higher injection rate, and a lower concentration of the CdSe core. (Large)core/crown NPLs were precipitated with ethanol and dispersed in hexane.

Synthesis of 4 ML Thick (Small)Core/Crown NPLs. Samples of 85 mg of $\text{Cd}(\text{myr})_2$ (mmol) and 7.5 mL of ODE were degassed into a three-neck flask. Under argon flow, the mixture is heated up to 230 °C. A total of 12 mg (0.15 mmol) of Se dispersed in 1 mL of ODE, prepared as described by Flamee et al.,³⁴ were injected. Thirty seconds after the Se injection, the anisotropic growth mixture was injected continuously in the three-neck flask at 30 mL/h. 4 ML thick (small)core/crown NPLs were precipitated with ethanol and dispersed in hexane.

Synthesis of 5 ML Thick (Small)Core/Crown NPLs. Samples of 85 mg of $\text{Cd}(\text{myr})_2$ (mmol) and 7.5 mL of ODE were degassed into a three-neck flask. Under argon flow, the mixture was heated up to 250 °C. A total of 12 mg (0.15 mmol) of Se dispersed in 1 mL of ODE, prepared as described by Flamee et al.,³⁴ were injected. Thirty seconds after the Se injection, the anisotropic growth mixture was injected continuously in the three-neck flask at 30 mL/h. 5 ML thick (small)core/crown NPLs were precipitated with ethanol and dispersed in hexane.

Optical Measurements of Ensemble of Core/Crown Nanoplatelets at Cryogenic Temperature. Core/crown nanoparticles were drop-casted on a sapphire substrate. The NPLs concentration was low with an optical density <0.1 at wavelength of >350 nm. The sample was mounted in an Oxford optistat CF-V continuous-flow cryostat where it was cooled by He vapor exchange gas. To reach cryogenic temperatures, the sample was subjected to a vacuum of less than 10^{-6} mbar. With this setup, the sample can be cooled to 10 K. Photoluminescence spectra and time-resolved fluorescence measurements over the temperature range 10–300 K were obtained using an Edinburgh FSP920 spectrometer. The sample was excited with an Edinburgh EPL375 laser diode with an emission wavelength at 376 nm or with a xenon 450 W arc lamp at 350 nm. The detector used for the experiment is an Edinburgh Instrument S900MCP microchannel plate.

Optical Measurements of Single Core/Crown Nanoplatelets. Core/crown NPLs in hexane solution were diluted to nanomolar concentration in a mixture of 90% hexane–10% octane and deposited by drop-casting on a glass substrate. The sample is visualized using an inverted fluorescent microscope. An area of the sample containing several NPLs is excited using a Hg lamp, and the emitted light is collected with an oil objective (Olympus 100 \times N.A. = 1.4) and adapted filters (560 SP for the excitation 590 LP for the emission). The emitted light of the sample can be observed on a charge-coupled device

camera (Cascade 512B, Roper Scientific) or directly through the microscope eyepiece. We record the fluorescence intensity emission of unique core/crown NPLs with a confocal microscope (Microtime 200, Picoquant) and a Hanbury Brown and Twist setup based on two avalanche photodiodes (SPAD PDM, MPD, time resolution 160 ps). The detected signal was recorded by a HydraHarp 400 module (Picoquant). In this configuration, the studied nanoparticle was excited with a pulsed diode emitting at 402 nm.

■ ASSOCIATED CONTENT

■ Supporting Information

Absorption, excitation, and emission spectra of a solution of core/crown NPLs and (small)core/crown NPLs with five monolayers thickness; core/crown NPLs TEM images; room-temperature photoluminescence spectrum of a typical single (small)core/crown NPL; emission and fluorescence lifetime evolution with temperature; and estimation of the energy gap between dark and bright state. This material is available free of charge via the Internet at <http://pubs.acs.org>.

■ AUTHOR INFORMATION

Corresponding Author

*E-mail: benoit.dubertret@espci.fr.

Notes

The authors declare no competing financial interest.

■ ACKNOWLEDGMENTS

We thank L. Biadala, B. Mahler, and C. Delerue for stimulating discussions and for valuable advice. We are grateful to X. Xu for performing TEM measurements. M.D.T. acknowledges the financial support of University Pierre et Marie Curie Paris 6. B.D. acknowledges Agence Nationale de la Recherche for funding.

■ REFERENCES

- (1) Murray, C. B.; Norris, D. J.; Bawendi, M. G. *J. Am. Chem. Soc.* **1993**, *115*, 8706–8715.
- (2) Manna, L.; Milliron, D. J.; Meisel, A.; Scher, E. C.; Alivisatos, A. P. *Nat. Mater.* **2003**, *2*, 382–385.
- (3) Peng, X.; Manna, L.; Yang, W.; Wickham, J.; Scher, E.; Kadavanich, A.; Alivisatos, A. *Nature* **2000**, *404*, 59–61.
- (4) Ithurria, S.; Tessier, M. D.; Mahler, B.; Lobo, R. P. S. M.; Dubertret, B.; Efros, A. L. *Nat. Mater.* **2011**, *10*, 936–941.
- (5) Joo, J.; Son, J. S.; Kwon, S. G.; Yu, J. H.; Hyeon, T. *J. Am. Chem. Soc.* **2006**, *128*, 5632–5633.
- (6) Smith, A. M.; Mohs, A. M.; Nie, S. *Nat. Nanotechnol.* **2009**, *4*, 56–63.
- (7) Hines, M. A.; Guyot-Sionnest, P. *J. Phys. Chem.* **1996**, *100*, 468–471.
- (8) Mahler, B.; Spinicelli, P.; Buil, S.; Quelin, X.; Hermier, J.-P.; Dubertret, B. *Nat. Mater.* **2008**, *7*, 659–664.
- (9) Chen, Y.; Vela, J.; Htoon, H.; Casson, J. L.; Werder, D. J.; Bussian, D. A.; Klimov, V. I.; Hollingsworth, J. A. *J. Am. Chem. Soc.* **2008**, *130*, 5026–5027.
- (10) Wang, X.; Ren, X.; Kahen, K.; Hahn, M. A.; Rajeswaran, M.; Maccagnano-Zacher, S.; Silcox, J.; Cragg, G. E.; Efros, A. L.; Krauss, T. D. *Nature* **2009**, *459*, 686–689.
- (11) Reiss, P.; Protière, M.; Li, L. *Small* **2009**, *5*, 154–168.
- (12) Mokari, T.; Banin, U. *Chem. Mater.* **2003**, *15*, 3955–3960.
- (13) Manna, L.; Scher, E. C.; Li, L.-S.; Alivisatos, A. P. *J. Am. Chem. Soc.* **2002**, *124*, 7136–7145.
- (14) Talapin, D. V.; Nelson, J. H.; Shevchenko, E. V.; Aloni, S.; Sadtler, B.; Alivisatos, A. P. *Nano Lett.* **2007**, *7*, 2951–2959.
- (15) De Mello Donegá, C. *Chem. Soc. Rev.* **2011**, *40*, 1512–46.
- (16) Mahler, B.; Nadal, B.; Bouet, C.; Patriarche, G.; Dubertret, B. *J. Am. Chem. Soc.* **2012**, *134*, 18591–18598.
- (17) Ithurria, S.; Talapin, D. V. *J. Am. Chem. Soc.* **2012**, *134*, 18585–18590.
- (18) Bouet, C.; Mahler, B.; Nadal, B.; Abecassis, B.; Tessier, M. D.; Ithurria, S.; Xu, X.; Dubertret, B. *Chem. Mater.* **2013**, *25*, 639–645.
- (19) Prudnikau, A.; Chuvilin, A.; Artemyev, M. *J. Am. Chem. Soc.* **2013**, *135*, 14476–14479.
- (20) Tessier, M. D.; Mahler, B.; Nadal, B.; Heuclin, H.; Pedetti, S.; Dubertret, B. *Nano Lett.* **2013**, *13*, 3321–3328.
- (21) Javaux, C.; Mahler, B.; Dubertret, B.; Shabaev, A.; Rodina, A. V.; Efros, A. L.; Yakovlev, D. R.; Liu, F.; Bayer, M.; Camps, G.; Biadala, L.; Buil, S.; Quelin, X.; Hermier, J.-P. *Nat. Nanotechnol.* **2013**, *8*, 206–212.
- (22) Nethercot, A. H. *Phys. Rev. Lett.* **1974**, *33*, 1088–1091.
- (23) Steiner, D.; Dorfs, D.; Banin, U.; Della Sala, F.; Manna, L.; Millo, O. *Nano Lett.* **2008**, *8*, 2954–2958.
- (24) Pandey, A.; Guyot-Sionnest, P. *J. Chem. Phys.* **2007**, *127*, 104710.
- (25) Benchamekh, R.; Even, J.; Jancu, J.-M.; Nestoklon, M.; Ithurria, S.; Dubertret, B.; Voisin, P. *20th Int. Symp. Nanostructures Phys. Technol. Russ. Federation, Nizhny Novgorod, Russia, June 24–30, 2012*.
- (26) Keldysh, L. *Sov. J. Exp. Theor. Phys.* **1979**, *29*, 716–719.
- (27) Van Sark, W. G. J. H. M.; Frederix, P. L. T. M.; Van Den Heuvel, D. J.; Gerritsen, H. C.; Bol, A. A.; Van Lingen, J. N. J.; De Mello Donegá, C.; Meijerink, A. *J. Phys. Chem. B* **2001**, *105*, 8281–8284.
- (28) Tessier, M. D.; Javaux, C.; Maksimovic, I.; Lorient, V.; Dubertret, B. *ACS Nano* **2012**, *6*, 6751–6758.
- (29) Labeau, O.; Tamarat, P.; Lounis, B. *Phys. Rev. Lett.* **2003**, *90*, 257404.
- (30) Biadala, L.; Louyer, Y.; Tamarat, P.; Lounis, B. *Phys. Rev. Lett.* **2009**, *103*, 037404.
- (31) Nirmal, M.; Norris, D.; Kuno, M.; Bawendi, M. *Phys. Rev. Lett.* **1995**, *75*, 3728–3731.
- (32) Lounis, B.; Bechtel, H. A.; Gerion, D.; Alivisatos, P.; Moerner, W. E. *Chem. Phys. Lett.* **2000**, *329*, 399–404.
- (33) Michler, P.; Imamoglu, A.; Mason, M.; Carson, P.; Strouse, G.; Buratto, S. *Nature* **2000**, *406*, 968–970.
- (34) Flamee, S.; Cirillo, M.; Abe, S.; De Nolf, K.; Gomes, R.; Aubert, T.; Hens, Z. *Chem. Mater.* **2013**, *25*, 2476–2484.